Fate and remnants of Majorana zero modes in a quantum wire array

Da Wang, Zhoushen Huang, and Congjun Wu
Department of Physics, University of California, San Diego, California 92093, USA
(Received 26 January 2014; published 20 May 2014)

Experimental signatures of Majorana zero modes in a single superconducting quantum wire with spin-orbit coupling have been reported as zero-bias peaks in tunneling spectroscopy. We study whether these zero modes can persist in an array of coupled wires, and if not, what their remnant might be. The bulk exhibits topologically distinct gapped phases and an intervening gapless phase. Even though the bulk pairing structure is topological, the interaction between Majorana zero modes and superfluid phases leads to spontaneous time-reversal symmetry breaking. Consequently, edge supercurrent loops emerge and edge Majorana fermions are in general gapped out except when the number of chains is odd, in which case one Majorana fermion survives.

DOI: 10.1103/PhysRevB.89.174510 PACS number(s): 03.65.Vf, 73.21.Hb, 74.25.−q, 71.10.−w

I. INTRODUCTION

Majorana fermions are intriguing objects because they are their own antiparticles. In condensed-matter physics, Majorana fermions arise not as elementary particles, but rather as superpositions of electrons and holes forming the zero-mode states in topological superconducting states. Majorana fermions were first proposed to exist in vortex cores and on boundaries of p-wave Cooper-pairing systems [1–3]. More recently, they were also predicted in conventional superconductors in the presence of strong spin-orbit (SO) coupling and the Zeeman field [4–9]. In cold atom physics, SO coupling has been realized by using atom-laser coupling [10–14]. This progress offers an opportunity to realize and manipulate Majorana fermions in a highly controllable manner, which has attracted a great deal of attention both theoretical and experimental [15–28].

Experimental signatures of Majorana zero modes have been reported as zero-bias peaks in the tunneling spectroscopy of a single quantum wire with strong SO coupling which either is coupled with an s-wave superconductor through the proximity effect [29–35], or is superconducting by itself [36]. A further study of an array of quantum wires is natural [26–28,37–42], in particular for the purpose of studying interaction effects among edge Majorana zero modes [26,43–45]. Topological states in an array of parallel wires in magnetic fields in the fractional quantum Hall regime have been studied recently [46,47]. Without imposing self-consistency, flat bands of Majorana zero edge modes have been found for uniform pairing as well as Fulde-Ferrell-Larkin-Ovchinnikov pairing [28,38–41], because under time-reversal (TR) symmetry these Majorana zero modes do not couple.

However, the band flatness of the edge Majorana zero modes is unstable due to interaction effects. Li, Wang, and Wu proposed the mechanism of spontaneous TR symmetry breaking for the gap opening in the edge Majorana flat bands [26]. Even in the simplest case of spinless fermions without any other interaction channels, the coupling between Majorana zero modes and the pairing phase spontaneously generates staggered circulating currents near the edge such that Majorana modes can couple to each other to open the gap due to the breaking of TR symmetry. Similar results were also obtained recently in Refs. [27,48]. The mechanism of gap opening based on spontaneous TR symmetry breaking also occurs in the helical edge modes of two-dimensional (2D) topological insulators under strong repulsive interactions, which leads to edge magnetism [49,50].

II. MAIN RESULTS

In this article, we investigate a coupled array of s-wave superconducting chains with intrachain SO coupling and an external Zeeman field. We consider both the proximity-induced and the intrinsic superconductivity. For the proximity-induced case, the array is placed on top of a bulk superconductor, and the phase coherence induces a nearly uniform pairing distribution in the quantum chains, $\Delta_{\boldsymbol{r}} = \Delta$. The bulk band structure exhibits several topologically distinct gapped phaseswith an intervening gapless phase. In the gapless phase, edge Majorana zero modes interpolate between nodes in the bulk energy spectrum. In the topological gapped phase, they extend into a flat band across the entire edge Brillouin zone. On the other hand, if either the phase coherence of the bulk superconductor is weak, or the superconductivity is intrinsic, as in the case of Pb nanowires [36] or cold atom systems near Feshbach resonance [18], then $\Delta_{\boldsymbol{r}}$ has to be solved self-consistently. We find that when the bulk is in the topological gapped phase, the phase distribution of pairing order parameters is inhomogeneous along the edge exhibiting TR symmetry breaking. It induces edge currents and gaps out the edge Majorana zero modes except when the chain number is odd, in which case one Majorana zero mode survives. If the bulk is in the gapless phase, in general TR breaking is also observed, but not always, because Majorana modes associated with opposite winding numbers can coexist on the same edge which can be coupled by TR-invariant perturbations.

III. MODEL OF QUANTUM WIRE ARRAY

Consider an array of SO coupled chains with the proximity-effect-induced s-wave pairing along the x direction, which are juxtaposed along the y direction. The band Hamiltonian is

$$\begin{aligned} H_0 = &-\sum_{\boldsymbol{r}\sigma} t(c^\dagger_{\boldsymbol{r}\sigma} c_{\boldsymbol{r}+\hat{x},\sigma} + \text{H.c.}) - \mu c^\dagger_{\boldsymbol{r}\sigma} c_{\boldsymbol{r}\sigma} \\ &- \sum_{\boldsymbol{r}} i\lambda (c^\dagger_{\boldsymbol{r}\uparrow} c_{\boldsymbol{r}+\hat{x},\uparrow} - c^\dagger_{\boldsymbol{r}\downarrow} c_{\boldsymbol{r}+\hat{x},\downarrow}) + \text{H.c.} \\ &- \sum_{\boldsymbol{r}\sigma} t_\perp (c^\dagger_{\boldsymbol{r}\sigma} c_{\boldsymbol{r}+\hat{y},\sigma} + \text{H.c.}), \end{aligned} \tag{1}$$

where $\boldsymbol{r}$ is the lattice site index; $\sigma = \uparrow, \downarrow$ labels two spin states; t and $t_\perp$ are intra- and interchain nearest-neighbor hoppings, respectively, and μ is the chemical potential. λ here is the SO coupling, which we choose to lie only in the x direction. This unidirectional SO coupling is a natural setup in cold atom experiments using atom-laser interaction [18,28]. The external field part of the Hamiltonian is

$$H_{ex} = \sum_{\boldsymbol{r}} \Delta_{\boldsymbol{r}}(c^\dagger_{\boldsymbol{r}\uparrow}c^\dagger_{\boldsymbol{r}\downarrow} + \text{H.c.}) - B(c^\dagger_{\boldsymbol{r}\uparrow}c_{\boldsymbol{r}\downarrow} + \text{H.c.}). \quad (2)$$

The first term accounts for superconducting pairing, where $\Delta_{\boldsymbol{r}}$ is the s-wave pairing on site $\boldsymbol{r}$, and can be induced either through the proximity effect or intrinsically. For the proximity-induced superconductivity, we take $\Delta_{\boldsymbol{r}}$ to be spatially uniform, which is a commonly used approximation. For intrinsic superconductivity, $\Delta_{\boldsymbol{r}}$ will be solved self-consistently. The second term arises from an external Zeeman field B, which can also be simulated using atom-laser coupling [18].

IV. UNIFORM PAIRING

Let us first consider a uniform pairing $\Delta_{\boldsymbol{r}} = \Delta$ which can be chosen as real without loss of generality. Under periodic boundary conditions in both x and y directions, the Hamiltonian Eqs. (1) and (2) can be written in momentum space,

$$H = H_{\text{band}} + H_{ex} = \sum_{\boldsymbol{k}} \psi^\dagger_{\boldsymbol{k}} h_{\boldsymbol{k}} \psi_{\boldsymbol{k}}, \quad (3)$$

where $\psi_{\boldsymbol{k}} = [c_{\boldsymbol{k}\uparrow}, c_{\boldsymbol{k}\downarrow}, c^\dagger_{-\boldsymbol{k}\uparrow}, c^\dagger_{-\boldsymbol{k}\downarrow}]^t$, and

$$h_{\boldsymbol{k}} = T_{\boldsymbol{k}}\tau_3 + \Lambda_{\boldsymbol{k}}\sigma_3 - B\sigma_1\tau_3 + \Delta\sigma_2\tau_2. \quad (4)$$

The two sets of Pauli matrices σ_i and τ_i $(i = 1,2,3)$ act in the spin and particle-hole spaces, respectively. $T_{\boldsymbol{k}}$ and $\Lambda_{\boldsymbol{k}}$ are given by

$$T_{\boldsymbol{k}} = -2t\cos k_x - 2t_\perp \cos k_y - \mu \quad (5)$$

and

$$\Lambda_{\boldsymbol{k}} = 2\lambda \sin k_x. \quad (6)$$

The energy spectrum of Eq. (4) is

$$E^2_{\boldsymbol{k}} = T^2_{\boldsymbol{k}} + \Lambda^2_{\boldsymbol{k}} + B^2 + \Delta^2 \pm 2\sqrt{T^2_{\boldsymbol{k}}\Lambda^2_{\boldsymbol{k}} + T^2_{\boldsymbol{k}}B^2 + B^2\Delta^2}. \quad (7)$$

Although h_{k_x,k_y} does not carry 2D topological indices, nevertheless we consider the 1D index of h_{k_x,k_y} at each fixed value k_y. It is invariant under both particle-hole (Ξ) and TR (Θ) symmetries: We define

$$\Xi = \tau_1, \quad \Theta = \sigma_1\tau_3, \quad (8)$$

and then

$$\Xi h_{k_x,k_y}\Xi^{-1} = -\Theta h_{k_x,k_y}\Theta^{-1} = -h^*_{-k_x,k_y}. \quad (9)$$

Here both transformations satisfy $\Theta^2 = \Xi^2 = 1$. We should emphasize here that Θ is *not* the physical time reversal, which should square to -1 for fermions with a half-integer spin. Here Θ is called "time reversal" because it represents a symmetry operation which is antiunitary and relates $\boldsymbol{k}$ to $-\boldsymbol{k}$. Θ and Ξ can be combined into a chiral symmetry defined as

$$\mathcal{C} = \Xi\Theta, \quad (10)$$

which gives

$$\mathcal{C}h_{k_x,k_y}\mathcal{C}^{-1} = -h_{k_x,k_y}. \quad (11)$$

These symmetries put h_{k_x,k_y} at fixed k_y in the BDI class as defined in Ref. [51], as pointed out in Ref. [40], which is characterized by a k_y-dependent 1D topological index denoted as W_{k_y}. A unitary transformation is performed as

$$U = e^{i(\pi/4)\sigma_2}\, u\, e^{-i(\pi/4)\tau_1}, \quad (12)$$

where

$$u = \tfrac{1}{2}(\sigma_0 + \sigma_3) + \tfrac{1}{2}\tau_3(\sigma_0 - \sigma_3). \quad (13)$$

It transforms $h_{\boldsymbol{k}}$ into an off-diagonal form

$$U^{-1}h_{\boldsymbol{k}}U = \begin{bmatrix} 0 & A_{\boldsymbol{k}} \\ A^\dagger_{\boldsymbol{k}} & 0 \end{bmatrix}, \quad (14)$$

where

$$A_{\boldsymbol{k}} = \Delta\sigma_1 - i(T_{\boldsymbol{k}}\sigma_0 + \Lambda_{\boldsymbol{k}}\sigma_1 + B\sigma_3). \quad (15)$$

$W(k_y)$ is defined as the winding number of $\det A_{\boldsymbol{k}}$ in the complex plane as k_x sweeps a 2π cycle, viz. [40,52],

$$W_{k_y} = -\frac{i}{2\pi}\int_{k_x=0}^{2\pi}\frac{dz(\boldsymbol{k})}{z(\boldsymbol{k})} = \frac{1}{2}[\text{sgn}(M_+) - \text{sgn}(M_-)]\text{sgn}(\lambda\Delta), \quad (16)$$

where $z(k) = \det A_k/|\det A_k|$, in which

$$\det A_k = B^2 - T^2_k - (\Delta - i\Lambda_k)^2. \quad (17)$$

$M_\pm(k_y)$ are related to $\det A_{k_x,k_y}$ as

$$M_+(k_y) = \det A_{k_x=0,k_y}, \quad (18)$$

$$M_-(k_y) = \det A_{k_x=\pi,k_y}. \quad (19)$$

$W_{k_y} = \pm 1$ requires the condition of $M_+(k_y)M_-(k_y) < 0$, and then $h(k_y)$ is topologically nontrivial. W_{k_y} changes discretely if a gap closing state appears on the line of k_y such that $M_+(k_y) = 0$, or $M_-(k_y) = 0$. The momenta of these states (k_x,k_y) satisfy the requirement that $k_x = 0$ or π, and another condition $T^2_k + \Delta^2 - B^2 = 0$ which determines k_y.

Based on W_{k_y}'s behavior over the range of $[-\pi,\pi)$, we plot the bulk phase diagram for the 2D Hamiltonian Eqs. (1) and (2) in the parameter plane μ-B shown in Fig. 1(a). The gapped phases are characterized by k_y-independent values of W: two phases with $W = \pm 1$ are weak topological pairing states, and the other two with $W = 0$ are trivial pairing states. For the gapless phase, a momentum-averaged topological number is defined as

$$r = \int \frac{dk_y}{2\pi} W_{k_y}. \quad (20)$$

The values of W_{k_y} vs μ and k_y are depicted in Fig. 1(b) along the line cuts L_1–L_5 in Fig. 1(a). Usually, W_{k_y} changes the value by only 1 at one step on varying k_y, but along the line

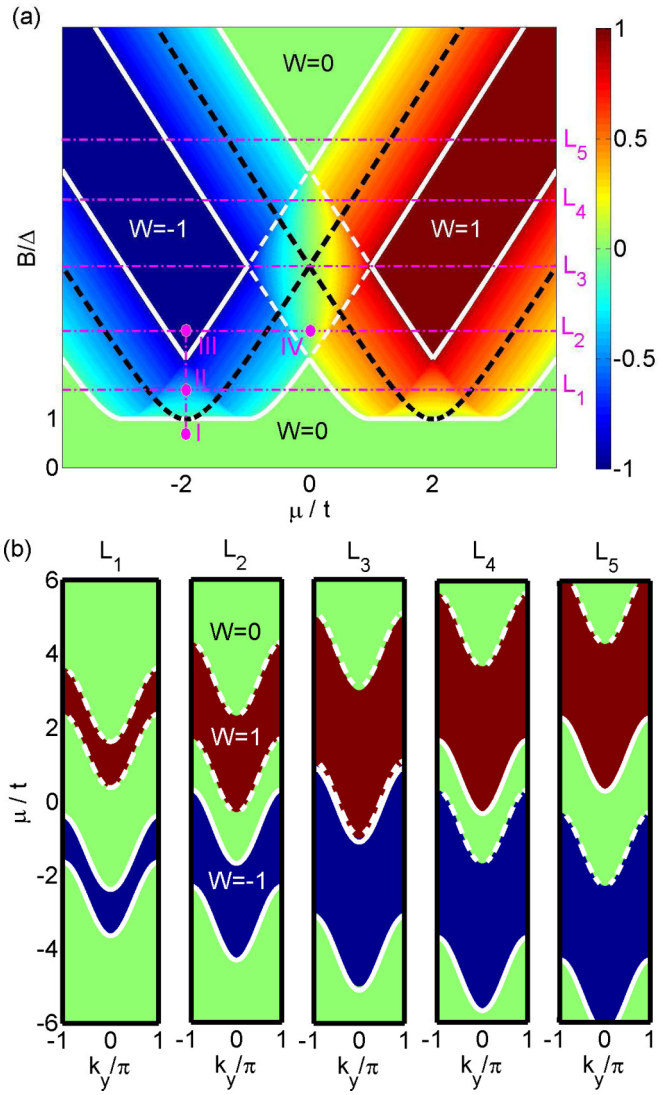

FIG. 1. (Color online) Bulk phase diagram of the 2D Hamiltonian Eqs. (1) and (2) in the μ-B plane with $B > 0$; that with $B < 0$ is symmetric with respect to the axis of $B = 0$. The parameter values are $t = 1$, $t_\perp = 0.5$, $\lambda = 2$, $\Delta = 0.5$. (a) The white solid lines enclose the gapless phase and separate the rest into two topologically trivial gapped phases and two nontrivial phases, respectively. Inside the gapless phase, states in the diamond enclosed by the white dashed lines exhibit edge modes associated with opposite winding numbers, and those outside the diamond exhibit only edge modes associated with the same winding number. The color scale encodes the momentum-averaged winding number r defined in Eq. (20). The gapless phase is suppressed as $t_\perp$ decreases, and it is compressed into the black dashed line at $t_\perp = 0$ (the single-chain limit). Points I–IV are used in Fig. 2. (b) W_{k_y} vs k_y and μ are shown along the lines of L_1–L_5 in (a), respectively. The white solid and dashed boundaries of the regions of $W_{k_y} = \pm 1$ represent that the gap closing points are located at $(0,k_y)$ and (π,k_y), respectively.

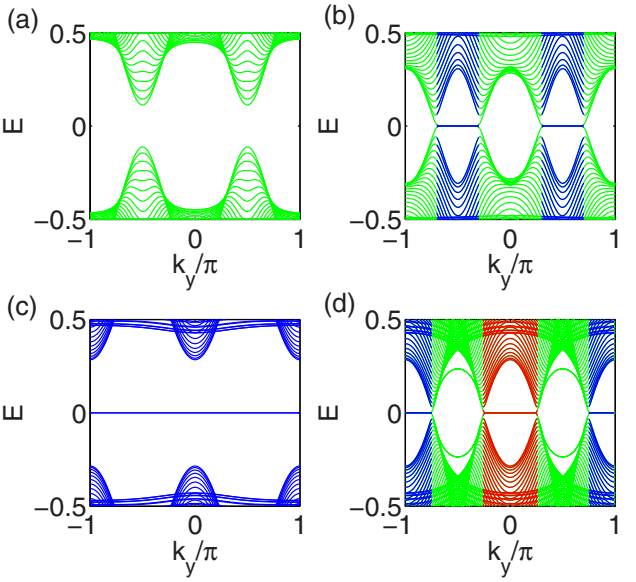

FIG. 2. (Color online) Edge spectra with open and periodical boundary conditions along the x and y directions, respectively. (a), (b), (c), and (d) correspond to points I, II, III, and IV marked in Fig. 1(a), respectively. (a) Gapped trivial phase; (b) gapless phase with edge modes associated with the same winding number; (c) gapped weak topological phase; (d) gapless phase with edge modes associated with opposite winding numbers. Parameters used are the same as those in Fig. 1(a).

L_3, W_{k_y} can directly change between 1 and -1 without passing 0, which means that two Dirac points $(0,k_y)$ and (π,k_y) appear at the same value of k_y. Note that the SO coupling λ is related to W_{k_y} only through its sign [cf. Eq. (16)]; therefore the phase diagram Fig. 1 is independent of λ (up to an overall sign flip).[1]

Next we discuss edge spectra in the above different phases. The open boundary condition is applied along the x direction. In the topological trivial phase shown in Fig. 2(a), the zero-energy edge modes are absent, while they appear and run across the entire 1D edge Brillouin zone in the gapped weak topological pairing phase shown in Fig. 2(b). In the gapless phase, flat Majorana edge modes appear in the regimes with $W(k_y) = \pm 1$ and terminate at the gap closing points [52–54]. These flat Majorana edge modes are lower dimensional Majorana analogues of Fermi arcs in 3D Weyl semi-metals [55]. This analogy goes further as in both cases the gapless phase intervenes between topologically distinct gapped phases.

The flat edge Majorana modes in the gapless phase can behave differently. In Fig. 2(b), all the edge flat Majorana modes are associated with the same value of W_{k_y}. In this case, these Majorana modes on the same edge are robust at zero energy if TR symmetry is preserved, which means that they do not couple. Nevertheless, TR symmetry may be spontaneously broken to gap out these zero modes [26]. On the other hand, for states inside the white dashed diamond in Fig. 1(a), edge Majorana modes appear with both possibilities of $W_{k_y} = \pm 1$. In particular, in the case of $\mu = 0$, the relation

[1]The value of λ determines the bulk gap in the topological superconducting regime. Therefore, for a given temperature T, $\lambda \gg T$ is required to observe this topological superconductivity physics.

$W(k_y) = -W(k_y + \pi)$ holds for edge Majorana modes as shown in Fig. 2(d). Majorana modes with opposite winding numbers on the same edge can couple to each other even without TR breaking, and thus are not topologically stable. r represents the net density of states of zero modes in the edge Brillouin zone which are stable under TR-conserved perturbations.

V. SELF-CONSISTENT SOLUTION

We now impose self-consistency on the pairing order parameter $\Delta_{\boldsymbol{r}}$, which is necessary for the case of intrinsic pairings. The pairing interaction is modeled as

$$H_\Delta = -g \sum_{\boldsymbol{r}} n_{\boldsymbol{r},\uparrow} n_{\boldsymbol{r},\downarrow}, \tag{21}$$

and the self-consistent equation is

$$\Delta_{\boldsymbol{r}} = -g \langle G | c_{\boldsymbol{r}\downarrow} c_{\boldsymbol{r}\uparrow} | G \rangle, \tag{22}$$

where $\langle G| \cdots |G\rangle$ means the ground-state average. We have verified numerically that $\Delta_{\boldsymbol{r}}$ is nearly uniform inside the bulk. Thus the bulk shares a phase diagram similar to that for uniform pairing (cf. Fig. 1), except that the values of Δ should be self-consistently determined.

Nevertheless, near edges $\Delta_{\boldsymbol{r}}$ varies spatially in the self-consistent solutions. If the bulk is in the topological gapped phase, the edge Majorana zero modes can couple with each other by breaking TR symmetry spontaneously as shown in Ref. [26]. Because of the band flatness, this effect is nonperturbative. This will gap out the zero Majorana modes and lower the edge energy. The system converges to an inhomogeneous distribution of $\arg[\Delta_{\boldsymbol{r}}]$ near the edges as shown in Fig. 3(a), even if this costs energy by disturbing the

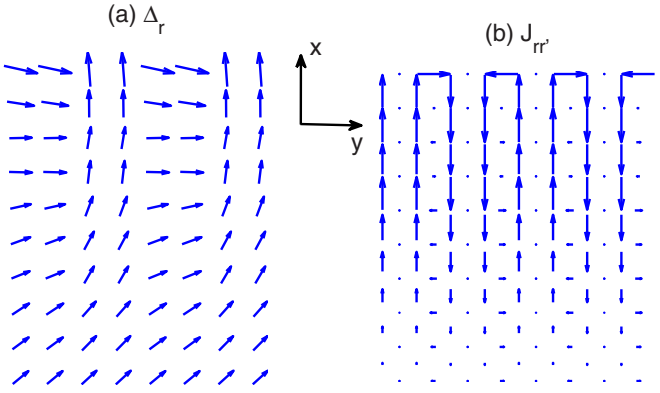

FIG. 3. (Color online) Self-consistent solutions for $\Delta_{\boldsymbol{r}}$ (a) and supercurrent $J_{\boldsymbol{r}\boldsymbol{r}'}$ (b). Parameter values are $L_x = 120$, $L_y = 8$, $B = 1.25$, $t = 1$, $t_\perp = 0.5$, $\mu = -2$, $\lambda = 2$, $g = 5$. Open and periodical boundary conditions are used along the x direction (vertical) and y direction (horizontal), respectively. Only the first ten sites from the upper edge are plotted. The distributions of $\Delta_{\boldsymbol{r}}$ and $J_{\boldsymbol{r}\boldsymbol{r}'}$ are reflection symmetric with respect to the center line of the system. (a) The direction and length of each arrow represent the phase and amplitude of $\Delta_{\boldsymbol{r}}$ on site $\boldsymbol{r}$. Its distribution is nearly uniform in the bulk but exhibits spatial variations near the edge. (b) Each arrow represents $J_{\boldsymbol{r}\boldsymbol{r}'}$ on bond $\boldsymbol{r}\boldsymbol{r}'$, which is prominent near the edge but vanishes in the bulk.

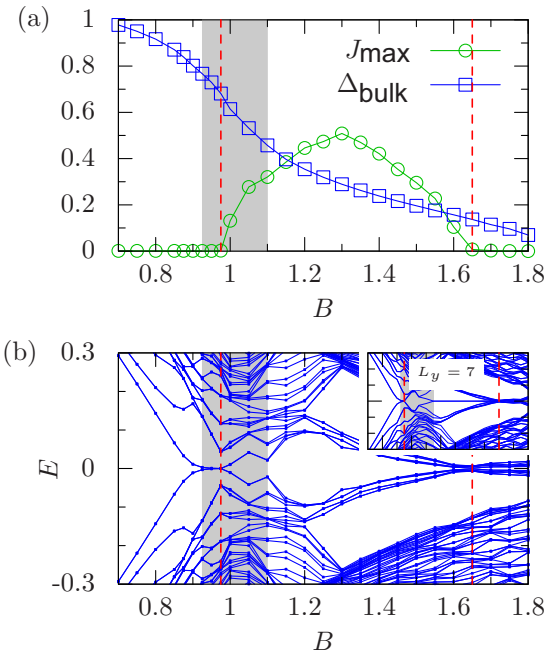

FIG. 4. (Color online) Self-consistent solutions for coupled chains with varying B field. Open and periodical boundary conditions are used along the x and y directions, respectively. Parameters are $L_x = 120$, $L_y = 8$, $t = 1$, $t_\perp = 0.5$, $\mu = -2$, $\lambda = 2$, and $g = 5$. In both (a) and (b), the bulk gapless phase is marked as the shaded region, which separates the topologically trivial (on its left) and nontrivial (on its right) gapped phases. (a) The bulk pairing Δ_{bulk} and the characteristic edge current magnitude J_{max} extracted as the maximal current in the system. (b) The energy spectra close to $E = 0$. The inset of (b) is for the case of $L_y = 7$. TR symmetry is spontaneously broken between the two dashed red lines as evidenced by $J_{\text{max}} \neq 0$. Please note that at large values of B, the edge current vanishes, which is an artifact due to the finite length of L_x. The decaying lengths of edge Majorana modes are on the order of the superconducting coherence length which is long due to the suppression of the pairing gap. As a result, Majorana modes on opposite edges can hybridize and are gapped out without breaking TR symmetry.

Cooper pairing [26]. This edge inhomogeneity in the pairing phase leads to an emergent current pattern as depicted in Fig. 3(b).

A natural question is under what conditions TR symmetry is spontaneously broken near edges. We have carried out extensive numerical studies and results for $\mu = -2$ are plotted in Figs. 4(a) and 4(b). TR symmetry is always broken in the topological gapped phase such that Majorana edge fermions are pushed to midgap energies, while TR symmetry remains unbroken in the trivial gapped phase. The latter is easy to understand because there are no Majorana fermions to begin with. If the bulk is in the gapless phase (shaded area in Fig. 4), the situation is more complicated. TR symmetry-breaking solutions are found in most of the gapless phase. In this regime, $|r| < 1$ and thus the number of stable Majorana modes on one edge is less than the number of chains L_y. These modes are associated with the same value of W_{k_y}, and thus TR symmetry breaking is needed to gap out these edge modes. There exists a small region inside the gapless phase in which TR symmetry

is unbroken in Fig. 4(a), which is largely due to the finite value of L_y. We have tested that on increasing L_y the TR breaking regime is extended, and thus we expect that it will cover the entire gapless phase in the thermodynamic limit. On the other hand, for the case of the gapless phase with $\mu = 0$ in which $r = 0$ for even values of L_y, our calculations show that all the Majorana modes are gapped out without developing currents. Instead a bond-wave order appears at the wave vector of $k_y = \pi$ along the edge, which is consistent with the fact that TR-invariant perturbations can destroy Majorana zero-energy modes at $r = 0$. In general, we expect that TR symmetry is spontaneously broken in the case of $r \neq 0$ in the thermodynamic limit.

However, not all Majorana edge modes have to be gapped out in the topological gapped phase. As shown in Fig. 4(b), for the case of $L_y = 8$, all the edge modes become gapped due to TR symmetry breaking, whereas for $L_y = 7$, one Majorana mode survives at zero energy.[2] The reason is that breaking TR symmetry brings the system from class BDI to class D [51], and the latter is characterized by a $\mathcal{Z}_2$ index. Physically it is because (in the infinite-chain-length limit) only the Majorana modes on the same edge can be paired and gapped out; thus, beginning with L_y Majorana fermions per edge, for odd L_y, one of them will always remain unpaired. In short, if TR is *spontaneously* broken, only $L_y$mod2 Majorana fermions per edge will persist at zero energy.

VI. DISCUSSION

Before closing, a few remarks are in order. (1) The phenomenon of spontaneous TR symmetry breaking in topological superconductors has previously been found in a spinless p-wave superconductor in Ref. [26]. Our work extends this observation in three ways: (a) Our results confirm that spontaneous TR breaking also occurs in a different setup with SO coupling and s-wave pairing, which is more relevant to experiments. (b) Our model hosts a gapless phase, wherein spontaneous TR breaking may also occur. (c) We also found a parameter regime where Majorana modes with opposite winding numbers can coexist. This provides another route to gap out the Majorana modes without invoking TR breaking. (2) In this work, we considered SO coupling only in the x direction, which can be exactly simulated in cold atom systems. However, in solid-state physics, both Rashba and Dresselhaus SO couplings will involve SO coupling along the y direction as well (unless Rashba and Dresselhaus SO coupling are of equal strength, in which case SO coupling along y will vanish). This will break TR symmetry [as defined in Eq. (8), which is not the usual physical TR symmetry] and bring the system from class BDI to D. In the presence of a y-direction SO coupling term [$\sim\sin(k_y)\sigma_2\tau_3$], the Majorana flat bands will develop dispersion, either connecting upper and lower bulk bands or forming isolated midgap states which may cross zero at $k_y = 0$ or π, consistent with a $\mathcal{Z}_2$ description [28,37]. (3) Disorders such as spatial variations of chemical potential ($\sim\sigma_0\tau_3$) and Cooper pairing amplitude ($\sim\sigma_2\tau_2$) can be added without changing any of our conclusions (provided the disorder is not strong enough to close the bulk gap). This is because these two terms are invariant under both particle-hole (Ξ) and TR (Θ) symmetries; hence the system still belongs to the BDI class. (4) Finally, although we modeled the constituent nanowires each as a 1D lattice, switching to a continuum formulation in the chain direction should not affect the formation of edge Majorana modes (that is, before they couple and gap out) [6,7]. Thus we expect the edge physics obtained here to be insensitive to how the bulk of the chains is formulated in terms of continuum vs lattice.

[2]The remaining Majorana mode is localized along the x direction, but delocalized along the y direction. A similar result can be found in Ref. [27].

VII. SUMMARY

We have studied quantum wire arrays with SO coupling and s-wave superconductivity in an external Zeeman field. The relation between edge Majorana zero modes and the bulk band structure is investigated in both topologically nontrivial gapped phases and the gapless phase. The coupling between Majorana modes and superfluid phases leads to spontaneous TR symmetry breaking. Our results have several experimental bearings. For proximity-effect-induced superconductivity, the number of edge Majorana fermions in the gapless phase can be tuned by the Zeeman field from zero all the way up to the number of chains. This could be detected as a prominent change in the height of zero-bias peaks in tunneling spectroscopy experiments. For the intrinsic superconductivity, edge supercurrent loops resulting from spontaneous TR breaking will induce small magnetic moments, which can be detected using magnetically sensitive experiments such as nuclear magnetic resonance or neutron scattering. The fluctuation in the number of persisting Majorana modes between 1 and 0, in the TR-broken topological gapped phase, may also show up in tunneling spectroscopy.

Note added. Recently, we became aware of a paper on a similar topic [37] and another related work [56].

ACKNOWLEDGMENTS

We thank Yi Li for early collaborations, Hui Hu and D. P. Arovas for helpful discussions, and D. P. Arovas for comments after reading a draft of this paper. D.W. and C.W. are supported by the NSF Grant No. DMR-1105945 and AFOSR Grant No. FA9550-11-1- 0067(YIP). Z.S.H. is supported by NSF through Grant No. DMR-1007028. C.W. acknowledges support from the NSF of China under Grant No. 11328403.

[1] G. Volovik, JETP Lett. **70**, 609 (1999).
[2] N. Read and D. Green, Phys. Rev. B **61**, 10267 (2000).
[3] A. Y. Kitaev, Phys. Usp. **44**, 131 (2001).
[4] L. Fu and C. L. Kane, Phys. Rev. Lett. **100**, 096407 (2008).
[5] R. M. Lutchyn, J. D. Sau, and S. Das Sarma, Phys. Rev. Lett. **105**, 077001 (2010).

[6] J. D. Sau, R. M. Lutchyn, S. Tewari, and S. Das Sarma, Phys. Rev. Lett. **104**, 040502 (2010).
[7] Y. Oreg, G. Refael, and F. von Oppen, Phys. Rev. Lett. **105**, 177002 (2010).
[8] J. Alicea, Phys. Rev. B **81**, 125318 (2010).
[9] L. Mao, M. Gong, E. Dumitrescu, S. Tewari, and C. Zhang, Phys. Rev. Lett. **108**, 177001 (2012).
[10] Y.-J. Lin, R. L. Compton, K. Jimenez-Garcia, J. V. Porto, and I. B. Spielman, Nature (London) **462**, 628 (2009).
[11] Y.-J. Lin, K. Jimenez-Garcia, and I. B. Spielman, Nature (London) **471**, 83 (2011).
[12] P. Wang, Z.-Q. Yu, Z. Fu, J. Miao, L. Huang, S. Chai, H. Zhai, and J. Zhang, Phys. Rev. Lett. **109**, 095301 (2012).
[13] L. W. Cheuk, A. T. Sommer, Z. Hadzibabic, T. Yefsah, W. S. Bakr, and M. W. Zwierlein, Phys. Rev. Lett. **109**, 095302 (2012).
[14] N. Goldman, G. Juzeliunas, P. Ohberg, and I. B. Spielman, arXiv:1308.6533.
[15] C. Zhang, S. Tewari, R. M. Lutchyn, and S. Das Sarma, Phys. Rev. Lett. **101**, 160401 (2008).
[16] M. Sato, Y. Takahashi, and S. Fujimoto, Phys. Rev. Lett. **103**, 020401 (2009).
[17] S.-L. Zhu, L.-B. Shao, Z. D. Wang, and L.-M. Duan, Phys. Rev. Lett. **106**, 100404 (2011).
[18] L. Jiang, T. Kitagawa, J. Alicea, A. R. Akhmerov, D. Pekker, G. Refael, J. I. Cirac, E. Demler, M. D. Lukin, and P. Zoller, Phys. Rev. Lett. **106**, 220402 (2011).
[19] M. Gong, G. Chen, S. Jia, and C. Zhang, Phys. Rev. Lett. **109**, 105302 (2012).
[20] K. Seo, L. Han, and C. A. R. Sá de Melo, Phys. Rev. Lett. **109**, 105303 (2012).
[21] R. Wei and E. J. Mueller, Phys. Rev. A **86**, 063604 (2012).
[22] X.-J. Liu and H. Hu, Phys. Rev. A **85**, 033622 (2012).
[23] X.-J. Liu, L. Jiang, H. Pu, and H. Hu, Phys. Rev. A **85**, 021603 (2012).
[24] A. Romito, J. Alicea, G. Refael, and F. von Oppen, Phys. Rev. B **85**, 020502 (2012).
[25] C. V. Kraus, M. Dalmonte, M. A. Baranov, A. M. Läuchli, and P. Zoller, Phys. Rev. Lett. **111**, 173004 (2013).
[26] Y. Li, D. Wang, and C. Wu, New J. Phys. **15**, 085002 (2013).
[27] T. Mizushima and M. Sato, New J. Phys. **15**, 075010 (2013).
[28] C. Qu, M. Gong, Y. Xu, S. Tewari, and C. Zhang, arXiv:1310.7557.
[29] V. Mourik, K. Zuo, S. M. Frolov, S. R. Plissard, E. P. A. M. Bakkers, and L. P. Kouwenhoven, Science **336**, 1003 (2012).
[30] M. T. Deng, C. L. Yu, G. Y. Huang, M. Larsson, P. Caroff, and H. Q. Xu, Nano Lett. **12**, 6414 (2012).
[31] A. Das, Y. Ronen, Y. Most, Y. Oreg, M. Heiblum, and H. Shtrikman, Nat. Phys. **8**, 887 (2012).
[32] L. P. Rokhinson, X. Liu, and J. K. Furdyna, Nat. Phys. **8**, 795 (2012).
[33] A. D. K. Finck, D. J. Van Harlingen, P. K. Mohseni, K. Jung, and X. Li, Phys. Rev. Lett. **110**, 126406 (2013).
[34] E. J. H. Lee, X. Jiang, R. Aguado, G. Katsaros, C. M. Lieber, and S. De Franceschi, Phys. Rev. Lett. **109**, 186802 (2012).
[35] E. J. H. Lee, X. Jiang, M. Houzet, R. Aguado, C. M. Lieber, and S. De Franceschi, Nat. Nanotechnol. **9**, 79 (2014).
[36] J. G. Rodrigo, V. Crespo, H. Suderow, S. Vieira, and F. Guinea, Phys. Rev. Lett. **109**, 237003 (2012); New J. Phys. **15**, 055020 (2013).
[37] I. Seroussi, E. Berg, and Y. Oreg, Phys. Rev. B **89**, 104523 (2014).
[38] R. M. Lutchyn, T. D. Stanescu, and S. Das Sarma, Phys. Rev. Lett. **106**, 127001 (2011).
[39] T. D. Stanescu, R. M. Lutchyn, and S. Das Sarma, Phys. Rev. B **84**, 144522 (2011).
[40] S. Tewari and J. D. Sau, Phys. Rev. Lett. **109**, 150408 (2012).
[41] M. Diez, J. P. Dahlhaus, M. Wimmer, and C. W. J. Beenakker, Phys. Rev. B **86**, 094501 (2012).
[42] G. Kells, V. Lahtinen, and J. Vala, Phys. Rev. B **89**, 075122 (2014).
[43] L. Fidkowski and A. Kitaev, Phys. Rev. B **81**, 134509 (2010).
[44] S. Ryu and S.-C. Zhang, Phys. Rev. B **85**, 245132 (2012).
[45] X.-L. Qi, New J. Phys. **15**, 065002 (2013).
[46] J. Klinovaja and D. Loss, Phys. Rev. Lett. **111**, 196401 (2013).
[47] J. Klinovaja and D. Loss, arXiv:1305.1569.
[48] A. C. Potter and P. A. Lee, Phys. Rev. Lett. **112**, 117002 (2014).
[49] C. Wu, B. A. Bernevig, and S.-C. Zhang, Phys. Rev. Lett. **96**, 106401 (2006).
[50] C. Xu and J. E. Moore, Phys. Rev. B **73**, 045322 (2006).
[51] A. P. Schnyder, S. Ryu, A. Furusaki, and A. W. W. Ludwig, Phys. Rev. B **78**, 195125 (2008).
[52] M. Sato, Y. Tanaka, K. Yada, and T. Yokoyama, Phys. Rev. B **83**, 224511 (2011).
[53] J. D. Sau and S. Tewari, Phys. Rev. B **86**, 104509 (2012).
[54] N. F. Yuan, C. L. Wong, and K. Law, Physica E **55**, 30 (2014).
[55] X. Wan, A. M. Turner, A. Vishwanath, and S. Y. Savrasov, Phys. Rev. B **83**, 205101 (2011); L. Balents, Physics **4**, 36 (2011).
[56] R. Wakatsuki, M. Ezawa, and N. Nagaosa, arXiv:1401.5192 [Phys. Rev. B (to be published)].